Solid State Communications 150 (2010) 794–798

Contents lists available at ScienceDirect

Solid State Communications

journal homepage: www.elsevier.com/locate/ssc

SiC/SiO_2 core–shell nanowires with different shapes: Synthesis and field emission properties

L.Z. Cao [a,b], H. Jiang [a,*], H. Song [a], X. Liu [a,b], W.G. Guo [a,b], S.Z. Yu [a,b], Z.M. Li [a], G.Q. Miao [a]

[a] Key Laboratory of Excited State Processes, Changchun Institute of Optics, Fine Mechanics and Physics, Chinese Academy of Sciences, Changchun 130033, PR China

[b] Graduate School of the Chinese Academy of Sciences, Beijing 100039, PR China

ARTICLE INFO

Article history:
Received 31 October 2009
Received in revised form
11 December 2009
Accepted 8 January 2010
by X.C. Shen
Available online 14 January 2010

Keywords:
A. SiC nanowires
B. Core–shell
C. Formation reason
D. Field emission characteristic

ABSTRACT

Three different shapes of SiC/SiO_2 core–shell nanowires were synthesized on Si substrates through a reaction between methane and silica using iron as catalyst. Analysis of scanning electron microscopy (SEM) and transmission electron microscopy (TEM) results indicated that catalyst morphology was the key factor for the formation of these three different products. The field emission properties of these three nanowires were investigated. Comparing the field emission results of these three nanowires, we can obtain a conclusion that a vertically well-aligned orientation to the substrate played a very significant role in improving the field emission properties when the emitters are up to a considerable number.

1. Introduction

Fabrication of one-dimensional (1D) (or quasi-one-dimensional) nanoscale materials with a specific size, morphology, and structure has attracted intensive research interest due to their importance in understanding the fundamental properties of 1D nanomaterials. As an important wide bandgap semiconductor, silicon carbide appears to be one of the most promising materials for blue and ultraviolet light emitting devices [1], and high power, high frequency electronic devices that can be operated at high temperatures and in harsh environments [2]. Recently, the quasi-one-dimensional SiC/SiO_x nanocables which could greatly enhance the emission intensity of SiC have been reported [3]. In addition, SiC nanowires have always been a research focus because of their high strength, low density, and high thermal stability that enables them to serve as a reinforcing phase in ceramic, metal, and polymer matrix composites [4]. In particular, the field emission properties of SiC nanowires and SiC/SiO_x nanocables have been studied and the results showed low turn-on and low threshold electric field values, which indicated that they could have potential applications in electron field-emitting devices [5,6].

So far, various SiC nanostructures including nanowires [5], nanocables [6], hollow nanospheres [7], nanoflowers [8], and nanosprings [9] have been synthesized using several approaches such as carbothermal reduction of sol–gel-derived silica xerogels [10], controlling the reaction between silicon halides and CCl_4 [11], laser ablation [12], arc-discharge [13], and chemical vapor deposition [14]. However, the simultaneous synthesis of three different SiC nanostructures by catalyst-assistant gas–solid reaction has rarely been reported.

In our previous work, the synthesis and study of the field emission properties of the 'aloetic-shaped' SiC nanowires have been reported [15]. In this paper, two other new different shapes of SiC/SiO_2 core–shell nanostructures, named as 'normal-shaped' and 'coralloid' nanowires were synthesized with the same growth conditions reported in our previous work. By comparing the characterized results, the reason for fabricating three different products is discussed. In addition, some effect factors on the field emission properties of SiC nanostructures are studied by comparing the field emission results of the different shapes of SiC nanowires.

2. Experimental

The SiC nanowires used in this study were synthesized via a catalyst-assistant gas–solid reaction [15]. In brief, 1 g SiO_2 (spectrally pure) and 0.8 g $FeCl_3 \cdot 5H_2O$ (analytically pure) powders were mixed with 5 ml deionized water. In order to obtain a uniform solution, the mixture was processed by a ball grinding mill with different times. Then the solution was spread uniformly over the surface of clean Si(100) substrates. After drying in a vacuum and annealing in a hydrogen atmosphere, the SiC nanowires were synthesized on Si substrates in a horizontal tube furnace system

* Corresponding author. Tel.: +86 431 8462 7073; fax: +86 431 8462 7073.
E-mail address: jiangh@ciomp.ac.cn (H. Jiang).

0038-1098/$ – see front matter © 2010 Elsevier Ltd. All rights reserved.
doi:10.1016/j.ssc.2010.01.008

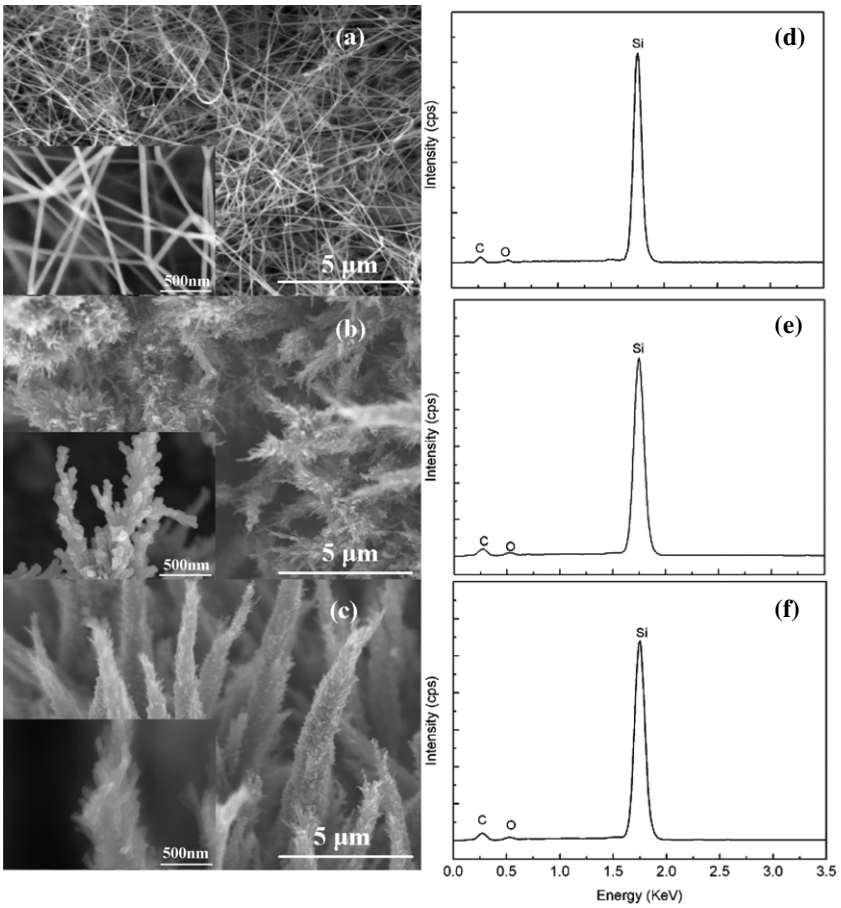

Fig. 1. (a) A SEM image of the normal-shaped SiC nanowires on a Si substrate. (b) A typical SEM image of the coralloid nanowires. (c) The general SEM image of the aloetic-shaped nanowires. Inset: High magnification SEM images of the corresponding nanowires. (d)–(f) EDX spectroscopy of the corresponding nanowires.

using methane (purity 99.99%) and hydrogen (purity 99.999%) with flow rates of 20 sccm and 50 sccm, respectively. The growth time was 10 min and the growth temperature was around 1250 °C at normal atmospheric pressure.

The as-grown nanowires were characterized by scanning electron microscopy (SEM, Hitachi S–4800), energy dispersive X-ray (EDX) spectroscopy, X-ray diffraction (XRD, Ricoh), and transmission electron microscopy (TEM, JEM–2010). Field emission experiments were carried out in a vacuum chamber with a base pressure $\sim 9 \times 10^{-5}$ Pa. The sample, as a cathode, was attached to a copper cylinder stand using conductive glue while the indium-tin-oxide (ITO)-coated glass was adopted as an anode. A quartz spacer of 500 μm thickness was placed on the substrate to isolate the cathode from the anode. The emission current was monitored by a picoammeter (Keithley 237).

3. Results and discussion

In Fig. 1(a), a typical SEM image of the normal-shaped SiC nanowires is shown. It can be seen that both straight and curved nanowires with a high density randomly grew on the Si substrate using the mixture treated for 1 h. The nanowires have a diameter of about 20–50 nm and a length of about 10 μm. The general SEM image of the coralloid-nanowires which grew on the Si substrate using the mixture treated for 10 min is displayed in Fig. 1(b). The nanowires have a tapered coralloid-structure with a diameter of about hundreds of nanometers and a length of about 10 μm. The surface and the tip of coralloid nanowires overgrew with smaller nanowires with diameters of about dozens of nanometers. Fig. 1(c) shows the SEM image of the aloetic-shaped nanowires growing with the untreated mixture. The insets of Fig. 1(a)–(c) are the high magnification SEM images of the corresponding nanowires. The EDX spectroscopy from the wire stem of the corresponding nanowires shows that the product contains only C, Si, and O, which is shown in Fig. 1(d)–(f). Quantitative analysis demonstrates that the C:Si:O atomic ratios of the normal-shaped, coralloid and aloetic-shaped nanowire are 41:47.05:11.95, 42.5:47.5:10 and 43.7:47.9:8.4, respectively. The fact that these elements coexist strongly suggests that the nanowires may have a SiC/SiO_2 core–shell structure, which will be proved by TEM measurements in detail.

The XRD pattern of these nanowires grown on a Si(100) substrate is shown in Fig. 2. Three peaks located at 35.7°, 41.4°, and 60° (2θ) are observed, which can be attributed to the diffraction of β-SiC (111), (200), and (220) planes, respectively. In addition, a strong diffraction peak of FeSi at 45.3° has been detected indicating that a FeSi phase was formed on the substrate surface [16]. The eutectic point of Fe and Si is about 1207 °C, so the FeSi phase may arise from the reaction between the Fe element and the Si substrate surface during the growth process [17].

With the aim of providing more information about the structure and crystallinity of the SiC nanostructures, TEM and HRTEM measurements are performed and the results are shown in Fig. 3. Fig. 3(a) shows a typical TEM image of the normal-shaped nanowires. It can be seen that the nanowires have a core–shell structure. The right part of Fig. 3(a) is the HRTEM image of the normal-shaped nanowire. The core has well defined fringes with a separation of 0.25 nm which is consistent with the d-spacing of (111) plane of β-SiC suggesting that the growth direction of nanowires is [111]. Together with the EDX analysis, we concluded

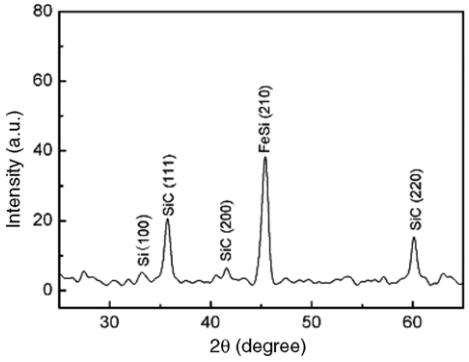

Fig. 2. A typical XRD pattern of SiC nanowires. The FeSi phase may be formed by the reaction between the Fe catalyst and Si substrate.

that the shell is amorphous SiO_2. Meanwhile, the smaller nanowire of the coralloid-nanowires and the aloetic-shaped nanowire both have a core–shell structure as shown in Fig. 3(c) and (d). The fabrication process of the core–shell structure has been described in detail in our previous work and the reaction process can be summarized as follows: First, when the temperature is up to 1250 °C, a carbonthermal reaction takes place and SiO vapor is formed. Second, the melted Fe combines with Si vapor, C or SiO to form liquid droplet alloys of Fe, Si, C and O. Third, as the CH_4 is continuously supplied, there will be a dense vapor of Si and C, and the Si and C in liquid droplets become supersaturated, and then the coexisting Si and C precipitate as nanowires. Finally, the unreacted SiO and O take place to form the amorphous SiO_2, which is then deposited on the SiC nanowires [18]. It is also seen that all of the three shapes of nanowires have a metal catalyst particle at the top as shown in Fig. 3(b)–(d).Thus, the growth mechanism of normal-shaped and coralloid SiC nanowires may also follow the "tip growth model" proposed by Amelinckx et al. [19]. It is known to all that the size and shape of the catalysts determine the size and shape of as-grown nanowires in the 'tip growth model'.

The reason for forming different products is not completely understood yet, but an explanation is presented here for discussion. In our experiment, the growth conditions are identical except for the ball grinding mill treating time of the SiO_2 and $FeCl_3$ mixture. It indicates that the treatment process is crucial for synthesizing different products. We assume that different treatment times will result in different catalyst morphologies (including the size and distribution of the particles). For the untreated mixtures, the catalyst particles are assembled together and their sizes are larger than the treated mixture after the annealing process in a hydrogen atmosphere. When the mixture is treated by a ball grinding mill within 10 min, the catalyst particles are assembled locally due to the fact that they were gradually dispersed. As the ball grinding mill treating time increased up to 1 h, the catalyst particles became uniformly dispersed. This assumption can be proved by the SEM images of the nanowires with a growth time of 10 s as shown in Fig. 4. Fig. 4(a)–(c) represent the SEM images of nanowires synthesized with the untreated mixture, the 10 min treated mixture, and the 1 h treated mixture, respectively. The catalyst morphology after the annealing process can be seen clearly in these images. At the same time, the growth trend of the nanowires can also be reflected by the catalyst's morphology. In Fig. 4(a), the catalyst particles are highly assembled and the aloetic-shaped nanowires may be formed on the large size and assembled catalyst particles. In Fig. 4(b), as-grown smaller nanowires are not dispersed but are assembled locally at the beginning of the growth process and this may be the reason for the formation of the coralloid nanowires. In Fig. 4(c), as-grown nanowires randomly grew on the substrate.

The characterizations of emission current versus voltage (I–V curves) of these three nanowires are shown in Fig. 5(a). The sample of the aloetic-shaped nanowires has a better I–V characterization which can be directly seen from the values of turn-on field and emission current density. The turn-on field (E_{to}) is defined as the electric field required to produce a current density of 10 μ A/cm^2. The turn-on fields of the normal-shaped, coralloid, and aloetic-shaped nanowires are around 1.56, 1.48, and 1.28 V/μm, respectively. The emission current density is mainly determined by the equation:

$$J = \frac{aE_{loc}^2}{\phi}\exp\left(-\frac{b\phi^{\frac{3}{2}}}{E_{loc}}\right)$$

where J is the emission current density, E_{loc} is the local electric field

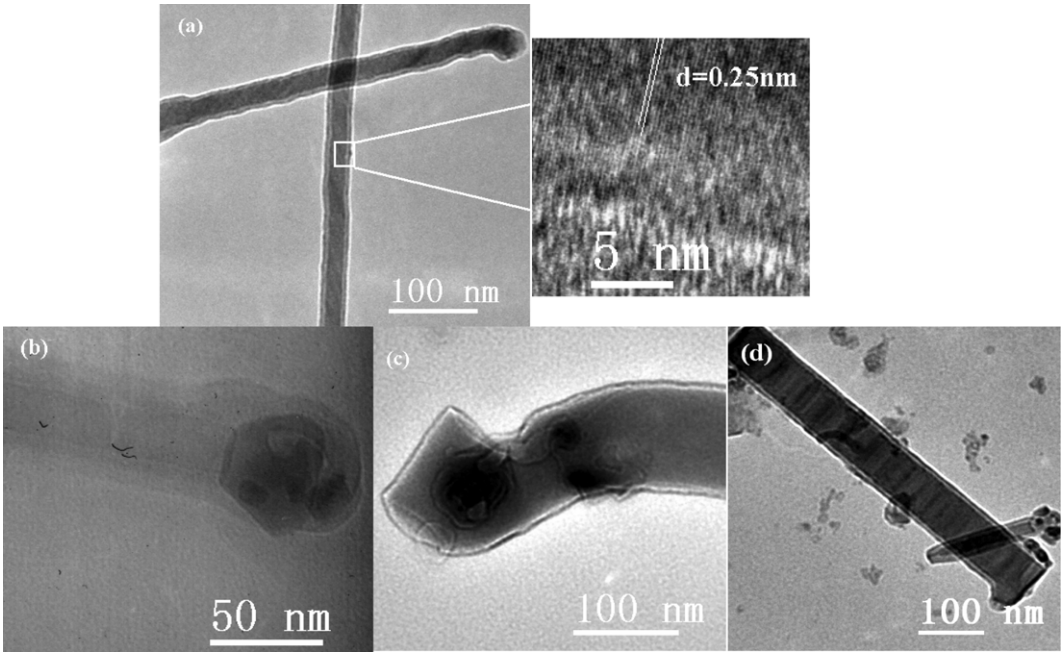

Fig. 3. (a) A typical TEM image of SiC/SiO_2 nanowires and the corresponding HRTEM image (right). (b) A typical TEM top image of a normal-shaped nanowire. (c) A typical TEM sub-nanowire image of a coralloid nanowire. (d) A typical TEM top image of an aloetic-shaped nanowire.

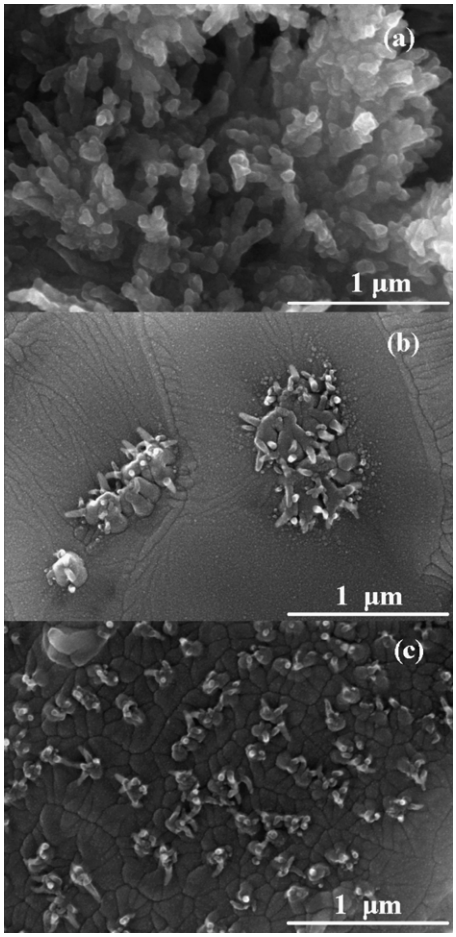

Fig. 4. The beginning SEM images of the nanowires synthesized with different treated time mixtures: (a) untreated, (b) 10 min and (c) 1 h.

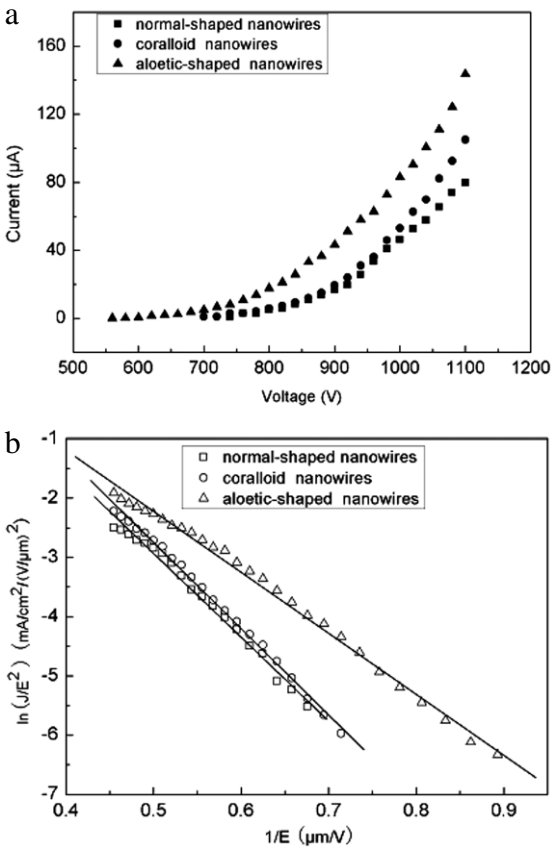

Fig. 5. (a) Current vs. voltage characteristics and (b) the corresponding Fowler–Nordheim plot of the nanowires. The straight solid line is the F–N fitting plot.

of the emitter top, Φ is the work function of the material, and a and b are constants. To a specified material, the emission current density is mainly determined by the applied electric field (E). With an applied low electrical field of 2.2 V/μm, the emission current density of the normal-shaped, coralloid, and aloetic-shaped nanowires can be up to 0.4, 0.53, and 0.72 mA/cm^2, respectively. The E_{to} and emission current density of our three samples are comparable to the corresponding values in the literature [5,6]. It is found that the field emission characteristics of the normal-shaped, coralloid, and aloetic-shaped nanowires were gradually improved. This may attribute to the decrease of the field-screening effect [20]. With the emitters up to a considerable number, vertically well-aligned orientation of emitters to the substrate can effectively decrease the field-screening effect of adjacent nanowires.

Field emission is usually modeled using the Fowler–Nordheim (F–N) theory [5]. The corresponding F–N characterizations of the data in Fig. 5(a) are shown in Fig. 5(b). The experimental data is in good agreement with the conventional F–N mechanism. In comparison with SiC nanowires not coated with a SiO_2 shell, it suggested that there are two reasons for the good field emission properties of these nanowires. One is that high density nanowires and thorns have more efficient electron emitting sites leading to better field emission properties. The other is the thin SiO_2 shell with a small electron affinity (0.6–0.8 eV). By coating with 10 nm SiO_2 shell, the field emission properties of SiC nanowire emitters can be enhanced [6]. Meanwhile, the wide-bandgap SiO_2 can act as a protective layer for SiC core nanowires. Taking into account the good field emission properties and the simple procedure of our synthesis, i.e., simple deposition process of catalysts, these three SiC based emitters should be a promising electron source for potential applications.

4. Conclusions

In summary, we have successfully synthesized three different shapes of SiC/SiO_2 core–shell nanowires through the reaction of methane and silica using iron as catalyst. The study found that the catalyst morphology is the key factor for synthesizing different shapes of SiC nanowires. The synthetic approach presented here opens a new route to fabricate other different shapes of nanostructures. The effects of orientation and a thin SiO_2 shell on the field emission properties of SiC nanostructures are studied. The field emission results show that these nanowires are all well-suited to field emission, and their good field emission properties indicate that these three shapes of nanowires could have potential applications in flat panel displays and electron field-emitting devices.

Acknowledgements

This work was supported by the National Natural Science Foundation of the China (60877007, 60571004), and the Science and Technology Ministry of China (2003CB314702).

References

[1] H. Morkoc, S. Strite, G.B. Gao, M.E. Lin, B. Sverdlov, M. Burns, Appl. Phys. A. 76 (1994) 1363.
[2] A. Fissel, B. Schroter, W. Richter, Appl. Phys. Lett. 66 (1995) 3182.
[3] X.M. Liu, K.F. Yao, Nanotechnology 16 (2005) 2932.
[4] P. Kim, C.M. Lieber, Science 286 (1999) 2148.

[5] S.Z. Deng, Z.B. Li, W.L. Wang, N.S. Xu, J. Zhou, X.G. Zheng, H.T. Xu, J. Chen, J.C. She, Appl. Phys. Lett. 89 (2006) 023118.
[6] Y.W. Ryu, Y.J. Tak, K. Yong, Nanotechnology 16 (2005) S370.
[7] G.Z. Shen, D. Chen, K.B. Tang, Y.T. Qian, S.Y. Zhang, Chem. Phys. Lett. 375 (2003) 177.
[8] D. Zhang, A. Alkhateeb, H. Han, H. Mahmood, D.N. Mcllroy, M.G. Norton, Nano. Lett. 3 (2003) 983.
[9] G.W. Ho, A.S.W. Wong, D.J. Kang, M.E. Welland, Nanotechnology 15 (2004) 996.
[10] G.W. Meng, L.D. Zhang, C.M. Mo, S.Y. Zhang, Y. Qin, S.P. Feng, H.J. Li, J. Mater. Res. 13 (1998) 2533.
[11] Q.Y. Lu, J.Q. Hu, K.B. Tang, Y.T. Qian, G.E. Zhou, X.M. Liu, J.S. Zhu, Appl. Phys. Lett. 75 (1999) 507.
[12] W.S. Shi, Y.F. Zhang, H.Y. Peng, N. Wang, C.S. Lee, S.T. Lee, J. Am. Ceram. Soc. 83 (2000) 3228.
[13] Y.B. Li, S.S. Xie, X.P. Zou, D.S. Tang, Z.Q. Liu, W.Y. Zhou, G. Wang, J. Cryst. Growth. 223 (2001) 125.
[14] H.L. Lai, N.B. Wang, X.T. Zhou, H.Y. Peng, C.K. Au, N. Wang, I. Bello, C.S. Lee, S.T. Lee, X.F. Duan, Appl. Phys. Lett. 76 (2000) 294.
[15] L.Z Cao, H. Jiang, H. Song, Z.M. Li, X. Liu, W.G. Guo, D.W. Yan, X.J Sun, H.F. Zhao, G.Q. Miao, D.B. Li, J. Nanosci. Nanotechnol. 10 (2010) 2104.
[16] JCPDS Cards: 74-1302, 86-0794.
[17] D.P. Yu, Q.L. Hang, Y. Ding, H.Z. Zhang, Z.G. Bai, J.J. Wang, Y.H. Zou, W. Qian, G.C. Xiang, S.Q. Feng, Appl. Phys. Lett. 73 (1998) 3076.
[18] T. Seeger, P. Redlich, M. Ruffhle, Adv. Mater. 12 (2000) 279.
[19] S. Amelinckx, X.B. Zhang, D. Bernaerts, X.F Zhang, V. Ivanov, J.B. Nagy, Science 265 (1994) 635.
[20] L. Nilsson, O. Groening, C. Emmenegger, O. Kuettel, E. Schaller, L. Schlapbach, H. Kind, J.-M. Bonard, K. Kern, Appl. Phys. Lett. 76 (2000) 2071.